Supramolecular Self-Assembly of Dimeric Dendrons with Different Aliphatic Spacers

Guichao Kuang,[†] Yan Ji,[†] Xinru Jia,*[,†] Erqiang Chen,[†] Min Gao,[†] Jiuming Yeh,[‡] and Yen Wei*[,§]

Beijing National Laboratory for Molecular Sciences, Key Laboratory of Polymer Chemistry and Physics of the Ministry of Education, College of Chemistry and Molecular Engineering, Peking University, Beijing 100871, China, Department of Chemistry, Chung Yuan Christian University, Chung-Li 32023, Taiwan, and Department of Chemistry, Drexel University, Philadelphia, Pennsylvania 19104

Received July 9, 2008. Revised Manuscript Received November 6, 2008

A series of low-molecular-mass organogelators (LMOGs), dimeric dendrons based on natural amino acids, glycine. and aspartic acid, with different aliphatic spacers have been synthesized and their self-assembly behavior and structure−property relationship have been studied. Transmission electron microscopy (TEM), atomic force microscopy (AFM), infrared spectroscopy (IR), and small-angle X-ray scattering (SAXS) were employed to characterize the self-assembled structures and to examine the effect of the length of aliphatic spacers on the gelation. It was found that all of the gels were thermoreversible and stable for more than half a year at room temperature. The dimeric dendrons with longer aliphatic spacers displayed enhanced gelation ability. The SAXS patterns of the xerogels **G2SnG2** ($n = 6$, 8, and 10) showed periodical reflections that could be attributed to the formation of a hexagonal columnar phase, whereas **G2S15G2** formed a lamellar structure. Hydrogen bonding and $\pi-\pi$ stacking interactions were evidenced by IR and fluorescence spectroscopy with pyrene as a probe, respectively. Moreover, the compounds **G2SnG2** not only acted as efficient organogelators but also self-organized into thermotropic liquid crystal, with the mesophase formation being correlated to the spacer length.

Introduction

As one of the most important types of supramolecular architectures, "physical gels" with the fibrillar networks could be obtained from various low-molecular-weight organogelators (LMOG).[1] Numerous interesting applications of these gels have been explored, such as the synthesis of templated materials,[2a] biomimetic materials,[2b] and microparticles.[2c,d] In general, most of the organogels are thermoreversible, that is, the fibers or network structures are destroyed upon heating but reformed during cooling.[3] The weak interactions such as hydrogen bonding, hydrophobic, $\pi-\pi$ stacking, van der Waals and/or metal-ion coordination interactions are proved to be the major driving forces to form supramolecular assemblies and subsequently three-dimensional network structures.[4] Specially, hydrogen bonding and $\pi-\pi$ stacking are considered as the most predominant forces to govern the gel-phase assemblies.[4c−e] However, before the full potential applications of organogels can be realized, there are still many basic questions yet to be answered.[5] It remains a challenge in the design of effective organogelators with indispensable and sufficient structures as well as in the development of better understanding of kinetic and rheological properties.[6]

During the last several years, dendrimers and/or dendrons as gelators have attracted much attention. A large number of new dendritic structures have been found to form gels,[7] because Newkome et al. first reported the dendritic gelators of bola-amphiphiles.[8] For example, Smith et al. highlighted the excellent examples of gelators based on lysine.[9] Moreover, both one-component and two-component dendritic gelators were mentioned in their studies. They systematically described the relationships between the gel formation and

* To whom correspondence should be addressed. E-mail: xrjia@pku.edu.cn (X.J.); weiyen@drexel.edu (Y.W.).
[†] Peking University.
[‡] Chung Yuan Christian University.
[§] Drexel University.

(1) (a) Terech, P.; Weiss, R. G. *Chem. Rev.* **1997**, *97*, 3133. (b) Abdallah, D. J.; Weiss, R. G. *Adv. Mater.* **2000**, *12*, 1237.
(2) (a) Jung, J. H.; Ono, Y.; Shinkai, S. *Chem.−Eur. J.* **2000**, *6*, 4552. (b) Hafkamp, R. J. H.; Kokke, P. A.; Danke, I. M.; Guerts, H. P. M.; Rowan, A. E.; Feiters, M. C.; Nolte, R.J. M. *Chem. Commun.* **1997**, 545. (c) Rees, G. D.; Robinson, B. H. *Adv. Mater.* **1993**, *5*, 608. (d) Bhattacharya, S.; Srivastava, A.; Pal, A. *Angew. Chem., Int. Ed.* **2006**, *45*, 2934.
(3) (a) George, M.; Weiss, R. G. *Langmuir* **2002**, *18*, 7124. (b) Esch, J. V.; Schoonbeek, F.; Loos, M. D.; Kooijman, H.; Spek, A. L.; Kellogg, R. M.; Fernga, B. L. *Chem.−Eur. J.* **1999**, *5*, 937.
(4) (a) Bao, C.; Lu, R.; Jin, M.; Xue, P. C.; Tan, C. H.; Xu, T. H.; Liu, G. F.; Zhao, Y. Y. *Chem.−Eur. J.* **2006**, *12*, 3287. (b) Yagai, S.; Iwashima, T.; Kishikawa, K.; Nakahara, S.; Karatsu, T.; Kitamura, A. *Chem.−Eur. J.* **2006**, *12*, 3984. (c) Song, B.; Wang, Z. Q.; Zhang, X.; Smet, M.; Dehaen, W. *Adv. Mater.* **2007**, *19*, 416. (d) Jung, J. H.; John, G.; Masuda, M.; Yoshida, K.; Shinkai, S.; Shimizu, T. *Langmuir* **2001**, *17*, 7229. (e) Yan, X. H.; Cui, Y.; He, Q.; Wang, K. W.; Li, J. B. *Chem. Mater.* **2008**, *20*, 1522.
(5) (a) George, M.; Weiss, R. G. *Acc. Chem. Res.* **2006**, *39*, 489. (b) Hanabusa, K.; Maesaka, Y.; Kimura, M.; Shirai, H. *Tetrahedron Lett.* **1999**, *40*, 2385. (c) Geiger, C.; Stanescu, M.; Chen, L.; Whitten, D. G. *Langmuir* **1999**, *15*, 2241.
(6) Van Esch, J. H.; Feringa, B. L. *Angew. Chem., Int. Ed.* **2000**, *39*, 2263.
(7) Hirst, A. R.; Smith, D. K. *Top. Curr. Chem.* **2005**, *256*, 237.
(8) (a) Newkome, G. R.; Baker, G. R.; Arai, S.; Saunders, M. J.; Russo, P.; Gupta, V. K.; Yao, Z.; Miller, J. E.; Bouilion, K. *J. Chem. Soc. Chem. Commun.* **1986**, *10*, 752. (b) Newkome, G. R.; Baker, G. R.; Arai, S.; Saunders, M. J.; Russo, P. S.; Theriot, K. J.; Moorefield, C. N.; Rogers, L. E.; Miller, J. E. *J. Am. Chem. Soc.* **1990**, *112*, 8458.

10.1021/cm801868b CCC: $40.75
Published on Web 01/05/2009

Scheme 1. Structures of the Dimeric Dendrons Prepared Using Standard DCC Coupling Method

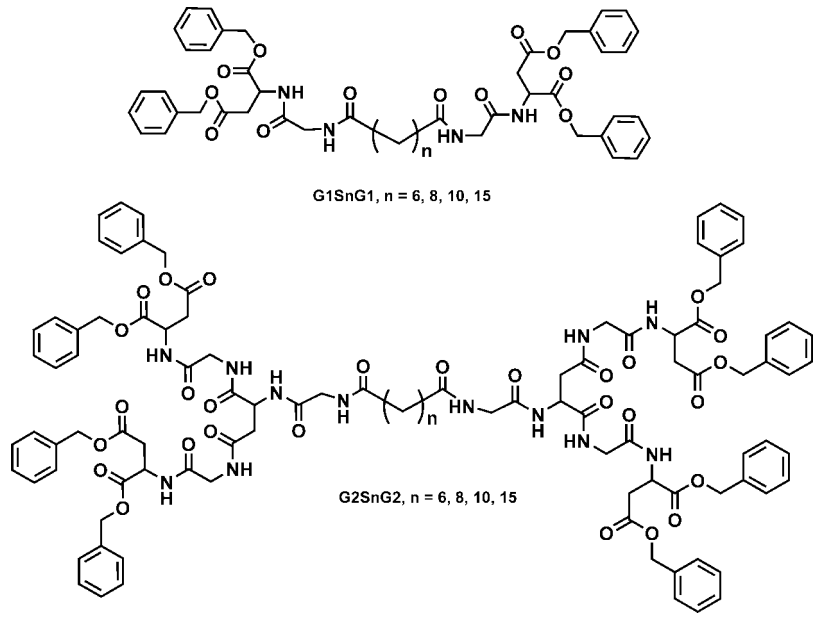

the related factors, including solvents, molecular chirality, dendritic generation, and peripheral structures. Aida et al. investigated the dendritic gelators composed of a peptidic core and Fréchet-type dendrons.[10] They reported that the dipeptide core, generation number and surface groups of dendrons played key roles in the gelation process.[10] Kim et al. reported the organogels from amide dendrons.[11] Chow et al. focused their studies on amino-acid-based gelators.[12] Stupp et al. showed that the dendron-rod-coil triblock structure molecules behaved as efficient gelators.[13] Very recently, Wang et al. demonstrated that a new type of amphiphilic diblock codendrimers could act as organogelators.[14] Percec and co-workers also reported the gels with thixotropic properties from the twin-dendritic gelators based on poly(benzyl ether) dendrons.[15]

In addition, dendrimers and/or dendrons behaving as liquid crystals (LCs) have also been an active field for continuing development.[16] Percec et al. elaborated the versatile LC properties of the poly(benzyl ether) dendrons and their derivatives.[17] Wiesner et al. reported that the mesophase behavior of macromolecular dumbbell was generation dependent,[18] that is, the second generation dumbbell-shaped molecules self-assembled into a hexagonal columnar mesophase, while those of third generation displayed a $Pm\bar{3}n$ arrangement. The self-assembly properties of molecular dumbbells with different dendritic wedges were also investigated by Lee et al.[19] They found that the aggregates displayed three-dimensional superlattice structures with tunable size.

However, little attention has been paid to the self-assembly of dendrimers and/or dendrons with combined features of both gel and LC. In our previous studies, we found that the dendrons made of natural amino acids, poly(Gly-Asp) dendrons, were capable of self-organizing into organogels in some organic solvents and lyotropic LC in benzyl alcohol.[20a,b] In this article, we describe the synthesis of a series of new dimeric dendrons with different aliphatic spacers as shown in Scheme 1. The influence of different aliphatic spacers on their self-assembly behavior and the structure−property relationship with respect to their gelation ability and thermotropic LC properties are also discussed.

Results and Discussion

Synthesis and Gel Preparation. The structures of the dimeric dendrons (**G1SnG1** and **G2SnG2** series) are shown in Scheme 1. These compounds were synthesized by standard DCC coupling of N-deprotected G2 dendrons and diacid with

(9) (a) Hirst, A. R.; Smith, D. K.; Feiters, M. C.; Geurts, H. P. M. *Langmuir* **2004**, *20*, 7070. (b) Love, C. S.; Hirst, A. R.; Chechik, V.; Smith, D. K.; Ashworth, I.; Brennan, C. *Langmuir* **2004**, *20*, 6580. (c) Partridge, K. S.; Smith, D. K.; Dykes, G. M.; McGrail, P. T. *Chem. Commun.* **2001**, 319. (d) Hirst, A. R.; Smith, D. K.; Feiters, M. C.; Geurts, H. P. M.; Wright, A. C. *J. Am. Chem. Soc.* **2003**, *125*, 9010. (e) Hirst, A. R.; Smith, D. K.; Feiters, M. C.; Geurts, H. P. M. *Chem. -Eur. J.* **2004**, *10*, 5901. (f) Smith, D. K. *Chem. Commun.* **2006**, 34. (g) Huang, B.; Hirst, A. R.; Smith, D. K.; Castelletto, V.; Hamley, I. W. *J. Am. Chem. Soc.* **2005**, *127*, 7130. (h) Smith, D. K. *Adv. Mater.* **2006**, *18*, 2773. (i) Hirst, A. R.; Huang, B. Q.; Castelletto, V.; Hamley, I. W.; Smith, D. K. *Chem.—Eur. J.* **2007**, *13*, 2180. (j) Hardy, J. G.; Hirst, A. R.; Ashworth, I.; Brennan, C.; Smith, D. K. *Tetrahedron* **2007**, *63*, 7397.

(10) (a) Jang, W. D.; Dong, D. L.; Aida, T. *J. Am. Chem. Soc.* **2000**, *122*, 3232. (b) Jang, W. D.; Aida, T. *Macromolecules* **2003**, *36*, 8461.

(11) (a) Kim, C.; Kim, k. T.; Chang, Y. *J. Am. Chem. Soc.* **2001**, *123*, 5586. (b) Ko, H. S.; Park, C.; Lee, S. M.; Song, H. H.; Kim, C. *Chem. Mater.* **2004**, *16*, 3872.

(12) (a) Chow, H. F.; Zhang, J. *Chem.—Eur. J.* **2005**, *11*, 5817.

(13) (a) Zubarev, E. R.; Pralle, M. U.; Sone, E. D.; Stupp, S. I. *J. Am. Chem. Soc.* **2001**, *123*, 4105. (b) Zubarev, E. R.; Sone, E. D.; Stupp, S. I. *Chem.—Eur. J.* **2006**, *12*, 7313, and references therein.

(14) Yang, M.; Zhang, Z. J.; Yuan, F.; Wang, W.; Hess, S.; Lienkamp, K.; Lieberwirth, I.; Wegner, G. *Chem.—Eur. J.* **2008**, *14*, 3330.

(15) Percec, V.; Peterca, M.; Yurchenko, M. E.; Rudick, J. G.; Heiney, P. A. *Chem.—Eur. J.* **2008**, *14*, 909.

(16) (a) Donnio, B.; Guillon, D. *Adv. Polym. Sci.* **2006**, *201*, 45. (b) Donnio, B.; Buathong, S.; Bury, I.; Guillon, D. *Chem. Soc. Rev.* **2007**, *36*, 1495.

(17) (a) Percec, V.; Cho, W. D.; Ungar, G.; Yeardley, D. J. P. *Chem.—Eur. J.* **2002**, *8*, 2011. (b) Percec, V.; Gloddde, M.; Peterca, M.; Rapp, A.; Schnell, I.; Spiess, H. W.; Bera, T. K.; Miura, Y.; Balagurusamy, V. S. K.; Aqad, E.; Heiney, P. A. *Chem.—Eur. J.* **2006**, *12*, 6298. (c) Percec, V.; Won, B. C.; Peterca, M.; Heiney, P. A. *J. Am. Chem. Soc.* **2007**, *129*, 11265.

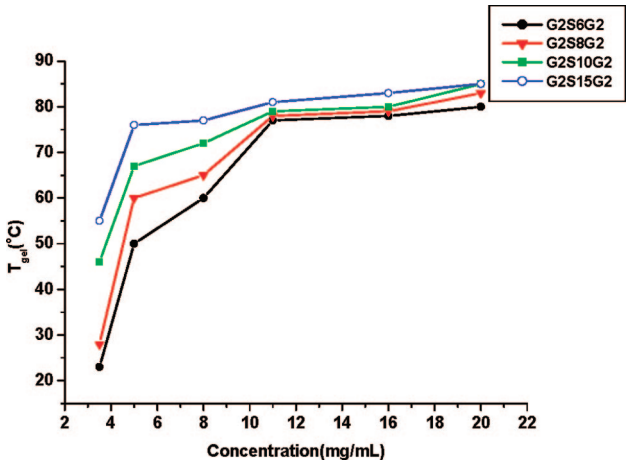

Figure 1. Plots of T_{gel} against gelator concentration in chloroform at a heating rate of 1 °C/min in water bath.

different aliphatic chains. The target compounds were readily obtained by precipitating the crude products in ethyl ether and methanol consecutively. NMR technique, matrix-assisted laser desorption/ ionization time-of-flight (MALDI-TOF) and elemental analyses were used to verify the structure and purity of the obtained compounds. The results are in good agreement with the proposed structures.

Gels were prepared with identical procedures. Taking **G2S6G2** as an example, a specific weight of **G2S6G2** was dissolved in chloroform in an ultrasonic bath, followed by gentle heating at 100 °C until a homogeneous and transparent solution was obtained. After being cooled to room temperature ($T \approx 25$ °C), the solution turned to gel in less than half an hour (0.2 wt %). This shows, for chloroform, that one molecule of **G2S6G2** can gel 7900 solvent molecules. However, except for dichloromethane and chloroform, none of other common solvents could be gelled by these compounds, which was in accordance with the gelation occurring exclusively in chlorinated solvents as reported by Tellado and co-workers.[21]

Thermal Stability of the Organogels. To gain better understanding of the influence of aliphatic spacers on gelation, the sol−gel temperature (T_{gel}), which is the transition temperature from an immobile to a mobile self-assembled state, was tested by tube inversion method. The compounds **G2SnG2** (n = 6, 8, 10, and 15) formed firm, translucent gels in a thermally reversible way at a concentration of 3.5 mg/mL in chloroform and maintained as gel for more than half a year at room temperature. But the series **G1SnG1** (n = 6, 8, 10 and 15) did not form gels in any organic solvents, which was contrary to the observation for the dimeric dendrons with lysine as the building blocks.[9g] As shown in Figure 1, the T_{gel} values, tested in a sealed tube (diameter ≈ 1 cm), appear in the order of **G2S15G2** > **G2S10G2** > **G2S8G2** > **G2S6G2**, indicating that the strength of organogels increased with the length of spacers. This result agreed well with those reported by Smith's group,[9a] but differed with that by Dordick et al.[22] whose gelators were found to display lower stability in ethyl acetate as the length of aliphatic chains was increased. The noncovalent forces, mainly hydrogen bonding and $\pi-\pi$ stacking between the dendritic headgroups, as well as van der Waals interactions are believed to be the primary factors determining the increase of T_{gel}. Additionally, the longer spacer could facilitate the solvation-assisted intermolecular arrangement, resulting in the dominating formation of fibers with high aspect ratio, which affords the stability to the gels.

Driving Force Analysis. The formation of gel phase assembly must be associated with the structural characteristics of phenyl units on the periphery and the amide groups in the dendritic branches.[20] The weak interactions as driving forces of the molecular subunits could include hydrogen bonding from amide branches, aromatic $\pi-\pi$ stacking between the phenyl rings, and the van der Waals interactions from the long alkyl chains. The evidence for the hydrogen bonding in the gel phase assemblies was that the gelled sample of **G2S6G2** changed into clear solution immediately by addition of a few drops of DMSO, a solvent known to be capable of breaking hydrogen bonds. The existence of hydrogen bonding was also supported by the fact that the gel of **G2S10G2** changed to solution by adding inorganic salt, LiCl, that could interact strongly with amide groups and break hydrogen bonds.[11a] FT-IR spectroscopy was employed for further establishing the existence of the hydrogen bonding. Using **G2S10G2** as an example, the signals at 3311, 1630, and 1541 cm^{-1} are assigned to the stretching vibrations of N−H, amide I and II bands in the gel state, respectively. These signals shifted to 3431, 1674, and 1521 cm^{-1} in solution, indicating the hydrogen bonding between N−H and C═O groups. In addition, pyrene was used as a probe to reveal the $\pi-\pi$ stacking between the phenyl rings.[20,23] It is well-known that the intensity ratio I_1/I_3 of pyrene emissions is an indicator for the polarity of microenvironment. It was found that the ratio decreased gradually with the increase in **G2S10G2** concentration (see the Supporting Information), which strongly supported that nonpolar microenvironment formed gradually by virtue of the $\pi-\pi$ stacking of the peripheral phenyl groups.

Structure of Gel Phase Assembly and Aggregation Mode. A combination of techniques consisting of transmission electron microscopy (TEM), atomic force microscopy (AFM), and small-angle X-ray scattering (SAXS) was used to elucidate the detailed microstructure of the assemblies from these dimeric dendritic gelators. Figure 2 shows the TEM images of dilute gel samples (c = 2 mg mL^{-1}) from **G2SnG2** (n = 6, 8, 10, and 15) with negative stained by uranyl acetate. Numerous intertwined fibers with 20−30 nm in width and several micrometers in length were observed.

(18) Cho, B. K.; Jain, A.; Gruner, S. M.; Wiesner, U. *Chem. Commun.* **2005**, 2143.
(19) Lee, M.; Jeong, Y. S.; Cho, B. K.; Oh, N. K.; Zin, W. C. *Chem.—Eur. J.* **2002**, *8*, 876.
(20) (a) Ji, Y.; Luo, Y. F.; Jia, X. R.; Chen, E. Q.; Huang, Y.; Ye, C.; Wang, B. B.; Zhou, Q. F.; Wei, Y. *Angew. Chem., Int. Ed.* **2005**, *44*, 6025. (b) Kuang, G. C.; Ji, Y.; Jia, X. R.; Li, Y.; Chen, E. Q.; Wei, Y. *Chem. Mater.* **2008**, *20*, 4173. (c) Li, W. S.; Jia, X. R.; Wang, B. B.; Ji, Y.; Wei, Y. *Tetrahedron* **2007**, *63*, 8794.
(21) Velázquez, D. G.; Díaz, D. D.; Ravelo, Á. G.; Marrero-Tellado, J. J. *Eur. J. Org. Chem.* **2007**, 1841.
(22) John, G.; Zhu, G. Y.; Li, J.; Dordick, J. S. *Angew. Chem., Int. Ed.* **2006**, *45*, 4772.
(23) Yumoto, M.; Kimura, M.; Shirai, H.; Hanabusa, K. *Chem.—Eur. J.* **2003**, *9*, 348.

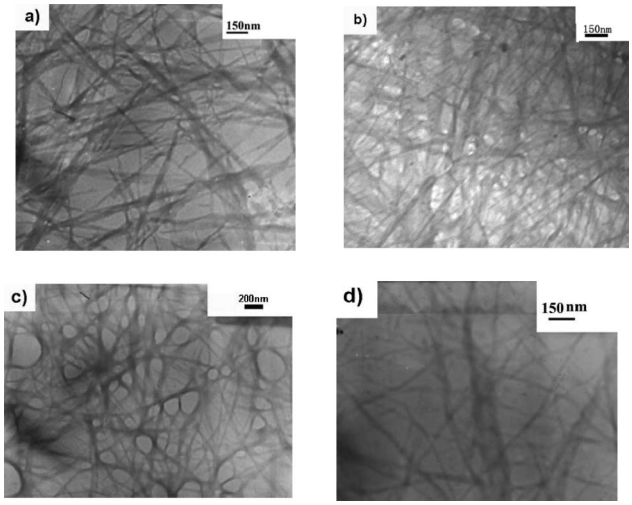

Figure 2. Negative stained (uranyl acetate) TEM images of (a) **G2S6G2**, (b) **G2S8G2**, (c) **G2S10G2**, and (d) **G2S15G2** made from chloroform (c = 2 mg/mL).

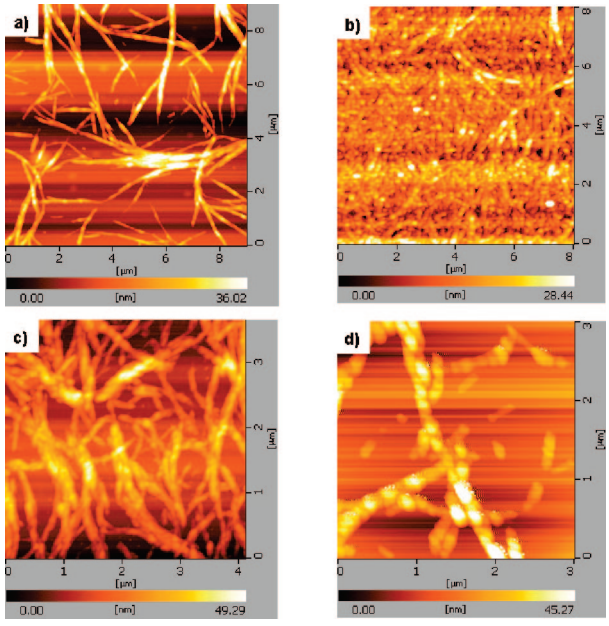

Figure 3. AFM images of the xerogel of (a) **G2S6G2**, (b) **G2S8G2**, (c) **G2S10G2**, and (d) **G2S15G2** made from chloroform (c = 5 mg/mL).

AFM images (c = 5 mg mL^{-1}), which were recorded in the tapping mode, depict that the diameter of bundled fibers was about 150−250 nm in width and approximately 30 nm in height (Figure 3). It is interesting to note that each fiber in AFM images is composed of a series of beads that are not found in the TEM images. However, we could not ascertain whether these "necklace-like" fibers,[24] clearly identifiable in AFM phase images, are helices or not (see the Supporting Information). The difference in size and morphology of the fibers between TEM and AFM images might be due to the hierarchical assembly with concentration-dependence during the gelation process.[10a,25] In the initial level, the molecules organize to nanofibers which are small as shown in the TEM images. These initial fibers grow further into "necklace" fibers with larger scale at higher concentrations. In a number

(24) Nagasawa, J.; Kudo, M.; Hayashi, S.; Tamaoki, N. *Langmuir* **2004**, *20*, 7907.

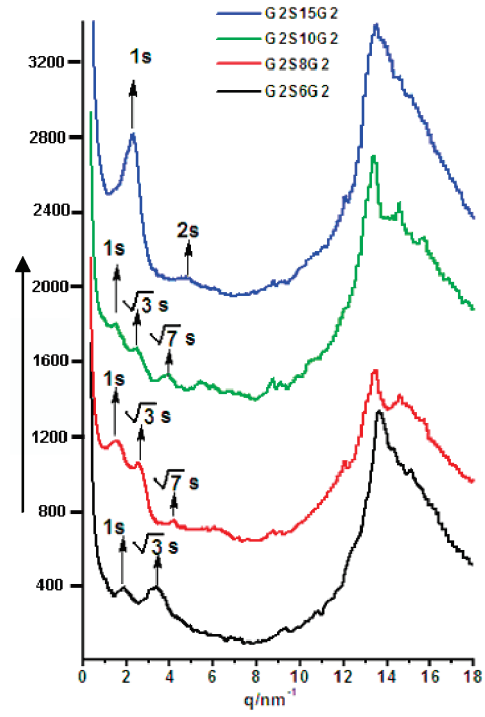

Figure 4. Powder SAXS patterns of the **G2SnG2** (n = 6, 8, 10, and 15) xerogels made from chloroform.

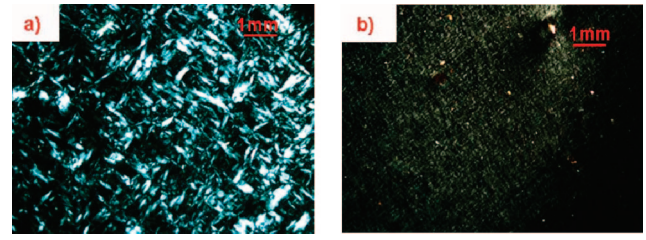

Figure 5. Polarized-light micrographs of (a) **G2S8G2** at 170 °C and (b) **G2S15G2** at 140 °C cooling from its clearing point, cooling rate 2 °C/min.

of pioneering works, the self-organization process with solvent-dependence was discussed. In our case, the organization process is clearly concentration-dependent, which is in agreement with the results by Meijer,[25a] Moore,[25b] Banerjee,[25c] and co-workers in their recent studies of pentapeptide-based organogelators.

Results obtained by SAXS were presented in Figure 4. The xerogels of **G2SnG2** (n = 6, 8, and 10) display three major diffraction peaks in the low angle region with the scatter vector ratio of 1:$\sqrt{3}$:$\sqrt{7}$. These values can be reasonably indexed as (100), (110), (210) diffractions. In the wide angle region, the asymmetric scattering halo could be divided into a narrow reflection peak and a broad halo that are centered at q = 13.4 nm^{-1} (d-spacing of 0.468 nm) and 14.4 nm^{-1} (d-spacing of 0.436 nm), respectively. These two reflection peaks are presumably attributed to crystal packing of rod segments within aromatic domains. Therefore, **G2SnG2** (n = 6, 8, and 10) most likely form the hexagonal columnar phase with the

(25) (a) Simmons, B. A.; Taylor, C. E.; Landis, F. A.; John, B. T.; McPherson, G. L.; Schwartz, D. K.; Moore, R. *J. Am. Chem. Soc.* **2001**, *123*, 2414. (b) George, S. J.; Ajayaghosh, A.; Jonkheijm, P.; Schenning, A. P. H.; Meijer, J. E. W. *Angew. Chem., Int. Ed.* **2004**, *43*, 3422. (c) Banerjee, A.; Palui, G.; Banerjee, A. *Soft Matter* **2008**, *4*, 1430.

Scheme 2. Proposed Process for the Hierarchical Molecular Organization of the Dimeric Dendrons in Chloroform: (a) MM2 Computed Structure for the Dimeric Dendrons in Space Filling Type, (b) Modeled Molecular Packing, (c) Fiber, (d) Fiber Bundles, (e) 3D Network, and (F) Gel Formed in Chloroform

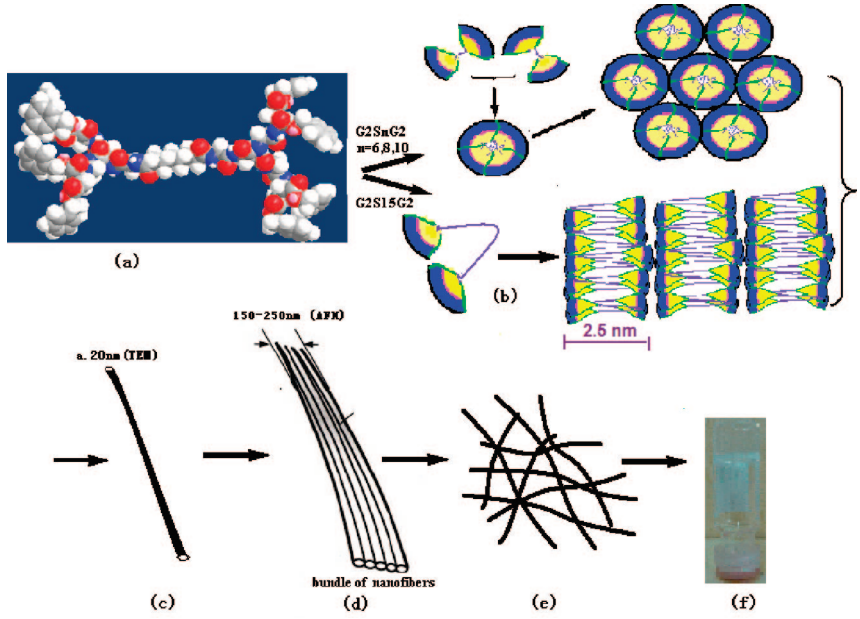

column diameter of 40.2, 42.9, and 44.6 Å, which are in good accordance with the CPK molecular modeling results. On the other hand, the xerogel of **G2S15G2**, the dimeric dendrons with a spacer of 15 carbons, showed a lamellar structure with the *d* spacing of 24.6 Å. This could be attributed to the adoption of a lamellar arrangement in the aggregates with long alkyl chains, which differed from the observations by Kim and co-workers on the architectures in xerogels related to the changing of aromatic bridging units between the dimeric dendrons.[11b] Because the fully extended length of **G2S15G2** is approximately 50.0 Å, the layer spacing ($d = 24.6$ Å) from the X-ray analyses is somewhat one-half of the calculated length of **G2S15G2** in extended conformation. Therefore, we postulate that the pairs of **G2S15G2** define the lamellar thickness in a folded-chain arrangement (Scheme 2), in which the dendritic headgroups overlap significantly via the hydrogen bonding and aromatic $\pi-\pi$ stacking.

On the basis of the above findings and discussions, we wish to propose a model for the self-organization of our dimeric dendrons as presented in Scheme 2 with the color yellow representing the amide structure and the color blue representing the benzyl groups. For **G2SnG2** ($n = 6$, 8, and 10), the molecules self-organize into assemblies with columnar hexagonal lattice, and then into elementary fibers. It can be seen that the amide groups link to each other to form intermolecular hydrogen bonding and the phenyl rings are close enough to form $\pi-\pi$ interactions. For **G2S15G2,** each molecule folds and packs into lamellar structure through aromatic $\pi-\pi$ stacking, hydrogen bonding and van der Waals interactions. Considering the calculated molecular length, a partially interdigitated arrangement of the dendritic headgroups is assumed in a lamellar space, as shown in Scheme 2. These fibers further aggregate into fiber bundles. The final process is that the fiber bundles grow and cross-link with each other to immobilize the solvent at macroscopic scale to form organogels. On the basis of such a model, the difference observed between the TEM and AFM images is, therefore, not altogether surprising.

Thermotropic Behavior. Usually, it has been considered impossible that low molecular weight compounds are capable of gelling solvents and displaying a thermotropic mesomorphic behavior at the same time till recent work by our group and a few others. We discovered that an amino-acid-based dendron could function as gelator and form lyotropic LC.[20a] Yagai et al. recently reported the dramatic change of self-organized structures by changing the length of alkyl linker between the dyes.[26] Li et al. reported that naphthalene derivatives could form gels in various solvents and also showed LC property.[27] Here, we present a very interesting observation that the dimeric dendrons, **G2SnG2** ($n = 6$, 8, 10, and 15), not only act as efficient organogelators but also self-organize into another important mesophase, i.e., thermotropic LC.

The LC behavior of **G2SnG2** was confirmed by the PLM observation on the first cooling (Figure 5), showing highly birefringent textures. However, this technique was not totally conclusive in giving unequivocal information concerning the assignment of the type of mesophase. To gain further insights into the LC behavior of these dumbbell molecules, DSC measurements were carried out. The second heating DSC traces (see the Supporting Information) show that both **G2S6G2** and **G2S8G2** melted at about 160 °C into a liquid crystalline state then transformed into the isotropic state at 192 and 190 °C, respectively. These results are consistent with the phase transition observed in PLM studies. However, for **G2S10G2** and **G2S15G2**, only one LC transition peak was observed during heating. An exothermic peak of LC

(26) Yagai, S.; Kinoshita, T.; Higashi, M.; Kishikawa, K.; Nakanishi, T.; Karatsu, T.; Kitamura, A. *J. Am. Chem. Soc.* **2007**, *129*, 13277.
(27) Yang, H.; Yi, T.; Zhou, Z. G.; Zhou, Y. F.; Wu, J. C.; Xu, M.; Li, F. Y.; Huang, C. H. *Langmuir* **2007**, *23*, 8224.

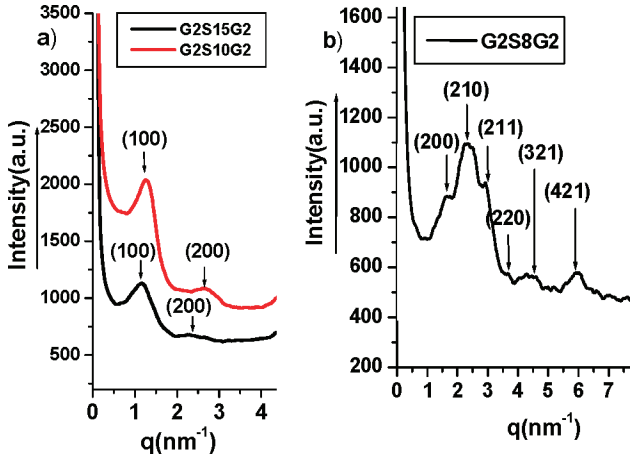

Figure 6. SAXS patterns of the mesophase of the dimeric dendrons: (a) **G2S10G2** at 150 °C and **G2S15G2** at 140 °C and (b) **G2S8G2** at 130 °C.

phase transition was observed for all of these compounds in the cooling traces. In contrast, the first generation systems, **G1SnG1** compounds, could not form LC phase. In addition, the mesophase of these compounds were identified by the temperature-dependent powder SAXS as shown in Figure 6. For **G2S10G2** and **G2S15G2,** lamellar architecture could be confirmed from the peaks in the low angle region and the first-order diffraction possesses the identical *d* spacing that are comparable to the extended conformation of the mesogen (Figure 6a). Contrary to the above-mentioned two compounds, the SAXS patterns of **G2S8G2** at different temperatures reveal that it self-organize into $Pm\bar{3}n$ lattices.[18,19] This observation is in agreement with that reported by Wiesner et al. who found that the molecular packing pattern is a function of generation of the dendrons but not the spacer length. For **G2S6G2,** we could not unambiguously identify the supramolecular structure from the SAXS patterns.

Conclusions

In summary, we have prepared a new series of dumbbell-shaped dimeric dendrons with different lengths of aliphatic spacers and studied their gelation ability and the structure−property relationship. The thermal and morphological properties were found to change significantly according to the size and shape of the dumbbell molecules. The **G2SnG2** (*n* = 6, 8, 10, and 15) compounds could self-assemble into fibrous networks, while **G1SnG1** (*n* = 6, 8, 10, and 15) could not. The relationships between the mesomorphic properties and gelation ability have also been investigated. Intermolecular hydrogen bonding, van der Waals force and aromatic $\pi-\pi$ stacking interaction between the phenyl rings were demonstrated to be the driving forces for the self-organization. A plausible hierarchical self-organization scheme is proposed. Moreover, the **G2SnG2** (*n* = 6, 8, 10, and 15) compounds not only form organogels but also self-organize into thermotropic LC phases, with strong dependence on the length of the spacers in both processes. We believe the compounds described here may have great potential for soft material applications. Further research along this line is currently in progress in our laboratory.

Experimental Section

Materials and Instrumentation. All reagents and common solvents were obtained from commercial sources and used as received unless otherwise stated. ^{1}H NMR and ^{13}C NMR spectra were recorded on Brucker 300 and 400 MHz spectrometers at room temperature using d_6-dimethyl sulfoxide and $CDCl_3$ as solvents and tetramethylsilane as an internal standard. Matrix-assisted laser desorption/ionization time-of-flight (MALDI-TOF) mass-spectra were acquired on a BIFLE XIII time-of-flight MALDI mass spectrometer with α-cyano-4-hydroxycinnamic acid (CCA) as the matrix, which was found to give the best resolution in our experiments. FT-IR spectra were obtained using a Bruker VECTOR22 IR spectrometer. Tapping-mode atomic force microscopy (AFM) measurement was performed using a SPA-400 multimode AFM and SPI3800N probe station. For the preparation of AFM samples, the rigid gel was dropped on a freshly cleaved mica surface and air-dried at room temperature before imaging. TEM images were obtained on a JEM-100 CXII microscope, operating at an acceleration voltage of 100 kV. The samples for TEM were prepared by depositing a gel formed in dilute chloroform on holey carbon film. SAXS measurements were performed on equipment with a SAXSess camera (Anton-Paar, Graz Austria), which was connected to an X-ray generator (Philips) operating at 40 kV and 50 mA employing Cu Kα radiation (λ = 0.154 nm). The 1D scattering functions (log $I(q)$) were obtained by integrating the 2D scattering pattern that was recorded on imaging-plate detector (Perkin-Elmer) using SAXSQuant software (Anton-Paar, Graz Austria). Gels were naturally dried for 2 days at room temperature and then dried at 50 °C in a vacuum oven for 5 h before SAXS experiment. DSC measurements were carried out on a Thermal Analysis Q100 DSC system. The fluorescence excitation and emission measurements were carried out at room temperature in chloroform using a Hitachi F-4500 fluorescence spectrophotometer.

Synthesis. The dendritic portions were synthesized according to the literature procedures.[20a] They were then used as reactants to be coupled with diacid by the standard DCC method to afford target dimeric dendrons.

Synthesis of **G1S6G1** *(*n = *6).* For the synthesis of **G1S6G1**, TFA-G1 (0.96 g, 2 mmol) was treated with N-methyl morpholine (1.5 mL) in a suitable volume of chloroform, and subsequently reacted with adipic acid (146 mg, 1 mmol) by adding cold solution of DCC dropwisely at −10 °C for 1 h. It was then taken into the refrigerator for 24 h. After filtration under reduced pressure to remove the DCU, the mixture was distilled under reduced pressure. The products were obtained with purification by silica gel column chromatography using ethyl acetate as the eluent.

Yield: 73%, ^{1}H NMR (300 MHz, $CDCl_3$, TMS, T = 298 K): δ 7.30−7.36 (m, 20H, Ar-*H*), 5.00−5.11 (s, 8H, COCH_2C$_6$H$_5$), 4.87−4.92 (t, 2H, NHC*H*CO), 3.88−3.94 (m, 4H, -NHCH_2CO), 2.87−3.10 (m,4H,-COCH_2CH), 2.66 (s, 2H), 1.70 (s, 2H). ^{13}C NMR: (75 MHz, $CDCl_3$, 298 K) δ 169.46−173.57 (CH$_2$*C*O), 135.00 (CH$_2$*C*$_6$H$_5$), 135.22 (CH$_2$*C*$_6$H$_5$), 128.18−128.56 (CH$_2$*C*$_6$H$_5$), 66.84−67.55 (OCH$_2$C$_6$H$_5$), 48.65 (NH*C*HCO), 42.89 (NH*C*H$_2$CO), 35.56−36.18 (*C*HCH$_2$CO), 24.56 (*C*H$_2$). Elemental Anal.: C, 64.93% (found 64.46%); H, 5.92% (found 5.80%); N, 5.92% (found 6.01%).

G1S8G1, **G1S10G1**, **G1S15G1** were synthesized following the same general procedure as that for the preparation of **G1S6G1**.

G1S8G1 (*n* = 8): Yield: 80%, ^{1}H NMR (300 MHz, $CDCl_3$, TMS, T = 298 K): δ .30−7.36 (m, 20H, Ar-*H*), 5.05−5.11(s, 8H, COCH_2C$_6$H$_5$), 4.88−5.01 (m, 2H, NHC*H*CO), 3.95−3.97 (m, 4H, NHCH_2CO), 2.89−3.10 (m, 4H, COCH_2CH), 2.23(m, 2H), 1.70 (s, 2H), 1.25 (s, 2H). ^{13}C NMR (75 MHz, $CDCl_3$, 298 K): δ 169.35−173.74 (CH$_2$*C*O), 135.98 (CH$_2$*C*$_6$H$_5$), 135.20 (CH$_2$*C*$_6$H$_5$),

128.22−128.59 ($CH_2C_6H_5$), 66.88−67.60 ($OCH_2C_6H_5$), 48.65 (NH-*C*HCO), 42.63 ($NHCH_2CO$) 35.46−36.17 (*C*HCH_2CO), 25.07 (*C*H_2), 27.88 (*C*H_2). Elemental Anal.: C, 65.59% (found 65.23%); H, 6.19% (found 6.02%); N, 6.37% (found 6.45%).

G1S10G1 (n = 10): Yield: 72%,^{1}H NMR (300 MHz, $CDCl_3$, TMS, T = 298 K): δ 7.28−7.38(m, 20H, Ar-*H*), 7.19−7.25 (d, 2H, N*H*CO), 6.46−6.48 (t, 2H, N*H*CO), 5.05−5.15 (d, 8H, $COCH_2C_6H_5$), 4.89−4.95 (m, 2H, NHC*H*CO), 3.88−3.99 (m, 4H, $NHCH_2CO$), 2.84−3.10 (m, 4H, -$COCH_2CH$), 2.23 (m, 2H), 1.70 (s, 2H), 1.25 (s, 4H). ^{13}C NMR (75 MHz, $CDCl_3$, 298 K): δ 169.03−173.72 (CH_2CO), 134.99 ($CH_2C_6H_5$), 135.21 ($CH_2C_6H_5$), 128.22−128.58 ($CH_2C_6H_5$), 66.87−67.58 ($OCH_2C_6H_5$), 48.63 (NH-*C*HCO), 42.90 ($NHCH_2CO$) 36.10−36.21 ($CHCH_2CO$), 28.69−28.89 (*C*H_2), 25.30 (*C*H_2). Elemental Anal.: C, 66.21% (found 66.37%); H, 6.45% (found 6.40%); N, 6.18% (found 6.03%).

G1S15G1 (n = 15): Yield: 65%, ^{1}H NMR (300 MHz, $CDCl_3$, TMS, T = 298 K): δ 7.23−7.36 (m, 20H, Ar−H), 7.19−7.25 (d, 2H, N*H*CO), 6.46−6.48 (t, 2H, N*H*CO), 5.05−5.11 (d, 8H, $COCH_2C_6H_5$), 4.90−4.94 (m, 2H, NHC*H*CO), 3.92−3.95 (m, 4H, $NHCH_2CO$), 2.85−3.09 (m, 4H, $COCH_2CH$), 2.17−2.22 (m, 4H), 1.15−1.63 (s, 7H), 1.26 (s, 22H). ^{13}C NMR (75 MHz, $CDCl_3$, 298 K): δ 168.99−173.66 (CH_2CO), 134.99 ($CH_2C_6H_5$), 135.21 ($CH_2C_6H_5$), 128.18−128.54 ($CH_2C_6H_5$), 66.82−67.53 ($OCH_2C_6H_5$), 48.64 (NH*C*HCO), 42.85 ($NHCH_2CO$) 36.19−36.25 (*C*HCH_2CO), 29.18−29.36 (*C*H_2), 25.50 (*C*H_2). Elemental Anal.: C, 67.60% (found 67.30%); H, 7.01% (found 6.90%); N, 5.73% (found 5.55%).

Synthesis of **G2S6G2.** For the synthesis of **G2S6G2**, TFA-G2 (0.5 g, 0.5 mmol) was treated with N-methyl morpholine (1.5 mL) in suitable volume of $CHCl_3$, and subsequently reacted with adipic acid (36 mg, 0.25 mmol) by adding cold solution of DCC dropwisely at −10 °C for 1 h. It was then taken into the refrigerator for 24 h. After filtration under reduced pressure to remove the DCU, the mixture was distilled under reduced pressure and the residue was treated ultrasonically in 400 mL of methanol to obtain the precipitates.

Yield: 53%. ^{1}H NMR (400 MHz, DMSO-d_6, TMS, T = 298 K): δ 7.32−7.35 (m, 40H, Ar-*H*), 5.06−5.08 (d, 16H, $COCH_2C_6H_5$), 4.75−4.79 (t, 4H, $COCH_2C_6H_5$), 4.58−4.60 (m, 2H, NHC*H*CO), 3.69−3.74 (m, 12H, $NHCH_2CO$), 2.50−2.94 (m, 12H, $COCH_2CH$), 2.12(s, 4H), 1.46 (s, 4H). ^{13}C NMR (100 MHz, DMSO-d_6, 298 K) δ 168.83−172.79 (CH_2CO), 156.61 (O*C*ONH) 135.72 ($CH_2C_6H_5$) 135.82 ($CH_2C_6H_5$), 127.67−128.46 ($CH_2C_6H_5$), 65.93−66.33 ($OCH_2C_6H_5$), 48.61−49.94 ($NHCH_2CO$), 33.36−37.30 ($CHCH_2CO$), 25.02−35.80 (CH_2). MALDI-TOF: $C_{98}H_{106}N_{12}O_{28}$ *m*/*z* calcd, 1898. Found: [M + Na], 1921; [M + K], 1937. Elemental Anal.: C, 61.95% (found 61.38%); H, 5.62% (found 5.55%); N, 8.85% (found 8.45%).

G2S8G2, **G2S10G2**, **G2S15G2** were synthesized following the same general procedures as that for the preparation of **G2S6G2**.

Synthesis of **G2S8G2** (n = 8): Yield: 48%. ^{1}H NMR (400 MHz, DMSO-*d6*, TMS, T = 298 K): δ 7.30−7.36 (m, 40H, Ar−H), 5.06−5.08 (d, 16H, $COCH_2C_6H_5$), 4.74−4.78(t, 4H, $COCH_2C_6H_5$), 4.57−4.59 (m, 2H, NHC*H*CO), 3.69−3.76 (m, 12H, $NHCH_2CO$), 2.49−2.90 (m, 12H, -$COCH_2CH$), 2.09−2.11(T, 4H), 1.44 (S, 4H), 1.20(s, 4H). ^{13}C NMR (100 MHz, DMSO-d_6, 298 K): δ 168.78−172.78 (CH_2CO), 156.61 (O*C*ONH) 135.70 ($CH_2C_6H_5$) 135.82 ($CH_2C_6H_5$), 127.68−128.46 ($CH_2C_6H_5$), 65.92−66.34 ($OCH_2C_6H_5$), 48.63−49.93 ($NHCH_2CO$), 33.33−37.36 ($CHCH_2CO$), 25.05−35.78(*C*H_2). MALDI-TOF: $C_{100}H_{110}N_{12}O_{28}$ *m*/*z* calcd, 1926. Found: [M + Na], 1949; [M + K], 1965. Elemental Anal.: C, 62.30% (found 61.85%); H, 5.75% (found 5.77%); N, 8.72% (found 8.62%).

Synthesis of **G2S10G2** (n = 10): Yield: 55%. ^{1}H NMR (400 MHz, DMSO-d_6, TMS, T = 298 K): δ 7.33−7.36 (m, 40H, Ar−H), 5.06−5.08 (d, 16H, $COCH_2C_6H_5$), 4.73−4.75 (t, 4H, $COCH_2C_6H_5$), 4.55−4.58 (m, 2H, NHC*H*CO), 3.69−3.71 (m, 12H, $NHCH_2CO$), 2.49−2.90 (m, 12H, -$COCH_2CH$), 2.08−2.10 (t, 4H), 1.44 (s, 4H), 1.20 (s, 8H).^{13}C NMR (100 MHz, DMSO-*d6*, 298 K): δ 69.44−173.75 (CH_2CO), 156.61 (O*C*ONH) 136.13 ($CH_2C_6H_5$), 136.00 ($CH_2C_6H_5$), 128.07−128.85 ($CH_2C_6H_5$), 66.30−66.70 ($OCH_2C_6H_5$), 48.91−50.26 ($NHCH_2CO$), 33.33−37.36 ($CHCH_2CO$), 25.43−35.98 (*C*H_2). MALDI-TOF: $C_{102}H_{114}N_{12}O_{28}$ *m*/*z* calcd, 1954. Found: [M + Na], 1977; [M + K], 1993. Elemental Anal.: C, 62.63% (found 62.08%); H, 5.87% (found 5.89%); N, 8.59% (found 8.22%)

Synthesis of **G2S15G2** (n = 15): Yield: 51%. ^{1}H NMR (400 MHz, DMSO-d_6, TMS, T = 298 K): δ 7.30−7.36 (m, 40H, Ar−H), 5.05−5.07 (d, 16H, $COCH_2C_6H_5$), 4.73−4.77 (t, 4H, $COCH_2C_6H_5$), 4.55−4.57 (m, 2H, NHCHCO), 3.68−3.75 (m, 12H, $NHCH_2CO$), 2.50−2.92 (m, 12H, -$COCH_2CH$), 2.08−2.11 (t, 4H), 1.44 (s, 4H), 1.20 (s, 10H).^{13}C NMR (100 MHz, DMSO-*d6*, 298 K): δ 168.92−172.94 (CH_2CO), 156.20 (O*C*ONH) 135.75 ($CH_2C_6H_5$) 135.89 ($CH_2C_6H_5$), 127.73−128.47 ($CH_2C_6H_5$), 65.88−66.27 ($OCH_2C_6H_5$), 48.57−50.02 ($NHCH_2CO$), 25.99−35.71 (*C*H_2). MALDI-TOF: $C_{104}H_{118}N_{12}O_{28}$ *m*/*z* calcd, 2025. Found: [M + Na]: 2048, [M + K]: 2064. Elemental Anal.: C, 63.43% (found 62.98%); H, 6.17% (found 6.08%); N, 8.30% (found 8.31%)

Acknowledgment. The research was funded by the National Natural Science Foundation of China (NSFC 20574001, 20640420562, and 20774003 to X.R.J.). Y.W. thanks the Chinese Ministry of Education and Li Ka-shing Foundation through the Chang-Jiang Scholar Program for support.

Supporting Information Available: FT-IR, CD, DSC, AFM phase images, pyrene probe test of the organogels, and SAXS diagrams of the xerogel (PDF). This material is available free of charge via the Internet at http://pubs.acs.org.

CM801868B